

1 Molecular characterisation of defence of *Brassica napus* (Oilseed rape) to *Rhizoctonia solani*

2 AG2-1 confirmed by functional analysis in *Arabidopsis thaliana*

3 Isabelle Sims¹, Dasuni Jayaweera¹, Kamal Swarup¹ and Rumiana V. Ray^{1*}

4

5 ¹Division of Plant and Crop Sciences, School of Biosciences, University of Nottingham, Sutton

6 Bonington Campus, Loughborough, Leicestershire, LE12 5RD

7

8 *Corresponding author: Rumiana.Ray@nottingham.ac.uk

9

10

11

12

13

14

15

16

17

18

19

20 Funding: The PhD of Isabelle L. Sims was funded by the BBSRC Doctoral Training

21 Programme at the University of Nottingham

22 **Abstract**

23 *Rhizoctonia solani* is a necrotrophic, soil-borne fungal pathogen associated with significant
24 establishment losses in *Brassica napus* (Oilseed Rape; OSR). The Anastomosis Group (AG)
25 2-1 of *R. solani* is most virulent to OSR, causing damping-off, root and hypocotyl rot, and
26 seedling death. Resistance to *R. solani* AG2-1 in OSR has not been identified, and the
27 regulation of OSR defence to its adapted pathogen, AG2-1, has not been investigated. In this
28 work, we used confocal microscopy to visualise the progress of infection by sclerotia of AG2-1
29 on *B. napus* varieties with contrasting disease phenotypes. We defined their defence response
30 using gene expression studies and functional analysis with *Arabidopsis thaliana* mutants. Our
31 results showed existing variation in susceptibility to AG2-1 and plant growth between OSR
32 varieties, and differential expression of genes of hormonal and defence pathways related to
33 auxin, ethylene, jasmonic acid, abscisic acid, salicylic acid, and reactive oxygen species
34 regulation. Auxin, abscisic acid signalling, and the MYC2 branch of jasmonate signalling
35 contributed to susceptibility to AG2-1, whilst induced systemic resistance was enhanced by
36 NAPDH RBOHD, ethylene signalling and the ERF/PDF branch of jasmonate signalling. These
37 results pave the way for future research, which will lead to the development of *Brassica* crops
38 that are more resistant to AG2-1 of *R. solani* and reduce dependence on chemical control
39 options.

40

41 **Keywords:** *Brassica napus*, *Rhizoctonia solani*, resistance, necrotroph, auxin, jasmonates,
42 ethylene

43

44 Introduction

45 *Brassica napus* L., known as oilseed rape (OSR), is a valuable crop species, primarily grown
46 for use as rapeseed oil, animal feed or biofuel. *Rhizoctonia solani* J.G. Kühn is a soil-borne,
47 fungal species complex divided into 13 reproductively isolated Anastomosis Groups (AGs)
48 (Carling et al. 2002), of which, AG2-1 is most virulent to *B. napus*. *R. solani* survives in the
49 soil as sclerotia (resting bodies of compacted mycelia), which in the presence of a susceptible
50 host, rapidly germinate to produce infectious hyphae colonising host tissues, and forming
51 infection cushions with hyphal pegs underneath to penetrate the host (Kataria and Verma
52 1992). On pre-germinated seedlings, symptoms of the developing damping off disease appear
53 as hypocotyl/root rot and necrotic lesions, although the pathogen is also known to inhibit seed
54 germination pre-emergence. Artificial inoculation of OSR with *R. solani* AG2-1 has shown a
55 reduction in establishment by 61% and a yield reduction of 41% (Jayaweera and Ray 2022).
56 Control is usually attempted through chemical and cultural methods, although there are
57 currently no approved chemical seed treatments, and genetic resistance has not yet been
58 identified (Brown et al. 2021; Jayaweera and Ray 2022).

59 Most of the information on the modulation of defence against *R. solani*, causing damping off,
60 has been provided by functional studies with the model plant, *Arabidopsis thaliana* (L.)
61 Heynh., challenged with AG8, or hypovirulent isolates of *R. solani* (Foley et al. 2013; Sharon
62 et al. 2011; Kumar et al. 2020; Kidd et al. 2021). Defence against *R. solani* AG8 has been
63 shown to involve jasmonic acid (JA) and ethylene (ET) pathways since mutations in JA (*coi1*),
64 ET (*ein2*, *ers1* or *ers2*) and *pen2* reduced plant survival under AG8 inoculation (Kidd et al.
65 2021). The NADPH oxidases (NOXs) double mutant *rbohD rbohF* was also highly susceptible
66 to *R. solani* AG8 (Foley et al. 2013; Kumar et al. 2020). In contrast to JA and ET responses to
67 AG8, auxin (Bartz et al. 2012) and ABA (Cordovez et al. 2017) mediated signalling pathways
68 have been identified as potentially increasing host susceptibility to various other AGs of *R.*

69 *solani*. Transcriptomics experiments showed that exposure to volatile organic compounds
70 released by *R. solani* AG2-2 IIIB induced upregulation of ABA and auxin signalling genes in
71 *A. thaliana*, while ET and JA signalling pathways were down-regulated (Cordovez et al. 2017).
72 Furthermore, isolates of AG1 IA, AG3 and AG4 have been shown to produce the auxin, phenyl
73 acetic acid (PAA) and its derivatives (Bartz et al. 2012; Iacobellis and DeVay 1987; Mandava
74 et al. 1980; Lakshman et al. 2006). PAA is a natural auxin with an overlapping regulatory role
75 with indole-3-acetic acid (IAA) (Sugawara et al. 2015) and in the host interaction with *R.*
76 *solani*, PAA production has been associated with increased disease severity on susceptible
77 hosts (Bartz et al. 2012). It is currently unknown if *R. solani* AG2-1 isolates produce PAA,
78 however the pathogen has been shown to produce IAA (Furukawa and Syono, 1998) suggesting
79 that these auxins play a role in the disease biology of OSR. Studies using hypovirulent
80 binucleate *Rhizoctonia* (Ru18-1, Ru89-1 [AG-B(o)], Rh521, and Ru56-8 (AG-A)) have
81 provided information on the early defence response to AG4 (HG-1), as increased expression of
82 genes PR5, PDF1.2, LOX2, LOX1, COR13 involved in induced systemic resistance and PAD3
83 of the phytoalexin production pathway was observed (Sharon et al. 2011). Whilst previous
84 studies with *A. thaliana* challenged by AG8 or hypovirulent *R. solani* have contributed to our
85 understanding of non-host defence regulation, further molecular studies are needed to define
86 the host-specific interactions in defence of OSR to AG2-1.

87 Here we provide new insights on OSR infection and the defence response to AG2-1 using
88 inoculation experiments with three contrasting OSR varieties and further functional studies
89 with *A. thaliana* mutants for key genes involved in hormonal regulation. This work aimed to
90 first quantify and characterise variation in the tolerance of small range of commercial varieties
91 of *B. napus* to *R. solani* AG2-1. We investigated this by quantifying disease symptoms and
92 root growth, as well as imaging the initial stages of the infection process with AG2-1 sclerotia.
93 Varieties with contrasting resistance responses were used for molecular characterisation to

94 identify differences in their defence pathways. We hypothesised that host susceptibility is
95 associated with increased expression of genes of the SA and auxin response, whilst enhanced
96 defence to AG2-1, like to AG8, with increased expression of genes of the JA and ET pathways.
97 We used RT-qPCR to investigate changes in gene expression and confirmed gene functionality
98 using *A. thaliana* mutant lines under inoculation with AG2-1.

99 **Materials and methods**

100 **Fungal inoculum preparation**

101 *R. solani* AG2-1 (isolate 1934 from the University of Nottingham isolate collection) was used
102 for inoculum production. AG2-1 was cultured on potato dextrose agar plates (PDA; Sigma-
103 Aldrich, UK) at room temperature (18°C). Inoculation was carried out using 6 mm diameter
104 AG2-1 cultured agar plugs from plates that were grown for 6-10 days before the production of
105 sclerotia. For microscopy experiments using sclerotia, plates were prepared in the same manner
106 and kept at room temperature for 4 weeks.

107 **AG2-1 inoculation in *Brassica napus***

108 Light expanded clay aggregate (LECA) particles were used for AG2-1 inoculation in *B. napus*
109 as roots of young seedlings were kept clean and intact for further analysis. This experiment
110 was carried out using a randomized block design, with 2 factors resulting in 10 treatment
111 combinations in 4 replications. The factors were: commercially available OSR variety
112 (Anastasia (LG seeds), Campus (KSW), SY Saveo (Syngenta), SY Sensia (Syngenta) or Skye
113 (Elsom seeds)) and pathogen inoculation (non-inoculated or AG2-1 inoculated). 40 pots (9 cm
114 in diameter) were filled one third with LECA particles (size 4-10mm; Saint-Gobain Weber
115 Limited, UK) and five either AG2-1 colonised (inoculated) or clean (non-inoculated) 6 mm
116 diameter PDA plugs before filling with the remaining two thirds of LECA particles. Seeds were
117 pre-germinated on filter paper in petri dishes with 5 ml sterile distilled water for three days in

118 the dark at room temperature (18°C). Three pre-germinated seedlings were added to each
119 LECA pot. The pots were supplemented with 25% Hoagland's (Sigma-Aldrich, UK) in 0.5 L
120 of purified water in equal amounts once only at the start of the experiment. Plants were kept in
121 a controlled environment chamber at 20°C with 12h photoperiod and a relative humidity of
122 60% under photosynthetically active radiation of 300 $\mu\text{mol m}^{-2} \text{s}^{-1}$.

123 **Disease assessment**

124 The symptoms of *Rhizoctonia* infection include damping-off, root rot and stem rot. The
125 hypocotyl and roots show necrotic lesions which become water soaked, soft and incapable of
126 supporting the plant. Disease assessment was conducted 7 days post inoculation using a scoring
127 scale of 0-4 for both hypocotyl and root; with 0 = symptomless, 1 = 25% symptoms, 2 = 50%
128 symptoms, 3 = 75% of symptoms, and 4 = plant death, modified from Drizou et al. (2017).
129 Root length was measured using photographs and the SmartRoot plugin for ImageJ (Schneider
130 et al. 2012; Lobet et al. 2011).

131 **Gene expression analysis**

132 Whole plant samples of *B. napus* were collected at 8, 24 and 48 hours post inoculation (hpi)
133 for RNA extraction, using RNeasy Plant kit (Qiagen) with TRIzol reagent (Invitrogen) as
134 described in Ajigboye et al. (2021). First strand cDNA was synthesized using iScript cDNA
135 Synthesis Kit (Bio-Rad). Quantitative reverse transcription PCR (RT-qPCR) with Sybr Green
136 (Bio-Rad) was conducted using CFX96 Touch Real-Time PCR Detection System (BioRad)
137 consisting of 95°C for 1 minute, followed by 40 cycles with 15 seconds at both 95°C and 60°C.
138 The primers are listed in supplementary Table S1. Relative quantification, with actin used as
139 the reference gene, for inoculated and non-inoculated plants (control) was calculated using the
140 $2^{-\Delta\Delta C_T}$ method (Livak and Schmittgen 2001). The disease-free, non-inoculated, plant samples
141 (control) were used as the calibrator, so that target gene expression can be interpreted relative

142 to the internal control in the inoculated plants compared with the non-inoculated (control)
143 plants (Schmittgen and Livak, 2008) allowing the calculation of fold change in gene expression
144 due to inoculation. Arithmetic means and standard errors were calculated with three biological
145 (each with three technical) replicates per sample.

146 **Wheat Germ Agglutinin (WGA)-Alexa Fluor/ Propidium Iodide staining and microscopy**

147 *B. napus* seedlings were surface sterilised for 8 minutes using a sterilisation solution containing
148 70% sodium hypochlorite (Parazone, Jeyes Limited, UK) and 0.2% Tween-20 and then washed
149 three times with sterile distilled water and plated on 10% (w/v) water agar. They were cold
150 stratified for 3 days then moved to a controlled environment room with 16h light at 21°C, 8h
151 dark at 15°C for 25 days. *R. solani* sclerotium were added next to (as close as touching) to the
152 roots of the plants to allow fast infection. Roots were sampled at 8, 24 and 48 hpi and stored in
153 100% ethanol to undergo bleaching upon collection. A minimum of 9 samples were examined
154 for each variety at each time point (average: 17). Ethanol was then replaced with 10%
155 potassium hydroxide and incubated at 85°C for 1.5 hours. Samples were washed five times in
156 phosphate buffer saline (PBS) pH7.4. Staining solution, made with 20µg/ml propidium iodide,
157 10µg/ml WGA-Alexa Fluor 488 conjugate (Thermo Fisher) and 0.1% (v/v) Tween-20 in PBS
158 pH7.4. Propidium Iodide was used to stain plant cell walls of root tissues and Alexa Fluor was
159 used to stain fungal hyphae. Vacuum infiltration at atmospheric pressure was completed 3
160 times for 5 minutes each with 5-minute intervals between them. Samples were washed twice
161 with PBS before visualisation with the Leica SP5 Confocal microscope (Leica Microsystems,
162 Germany) (Redkar *et al.* 2018).

163 **AG2-1 inoculation in *Arabidopsis thaliana***

164 *R. solani* AG2-1 is virulent to *A. thaliana*. Seeds of *A. thaliana* were obtained from NASC,
165 UK, Dr Ranjan Swarup and Dr Jorge Vicente Conde, University of Nottingham, and were

166 surface sterilised as above. The seeds were transferred to 50% MS pH 5.8 (Murashige and
167 Skoog Basal Medium, Sigma-Aldrich, UK), 1% agar plates and cold stratified at 4°C for 3
168 days. The plates were then moved to a controlled environment room with 16h light at 21°C, 8h
169 dark at 15°C and grown vertically for 11 days. Seedlings were transplanted into 3x4 well trays
170 containing a mix of M3 compost (Levington, Everris Limited, UK), vermiculite and perlite in
171 a 4:2:1 ratio. Three days later, the plants were transferred into experimental trays with 10 *R.*
172 *solani* AG2-1 colonised or non-inoculated 6 mm diameter PDA plugs per well added 3cm from
173 the top of the well. Trays were kept in a controlled environment chamber at 22°C with 16 h
174 photoperiod. Photographs were taken 11 days post inoculation, from above at constant distance,
175 using a digital camera and the green area for each plant was measured using ImageJ (Schneider
176 et al. 2012). A ruler was included in all photographs to set the scale for measurements.

177 **Infection and imaging of Jas9:VENUS plants**

178 *A. thaliana* Jas9:VENUS seeds were obtained from NASC (Stock code: N2105629) and were
179 surface sterilised, cold stratified, and grown on 50% MS pH 5.8 1% agar plates as described
180 above. After 8 days growth, *R. solani* mycelium from a PDA plate was added close to the plant
181 roots, and the plants were imaged 20 h after inoculation. Images were taken using a Leica SP5
182 Confocal microscope (Leica Microsystems, Germany).

183 **Infection and imaging of IAA2_{pro}:GUS plants**

184 *A. thaliana* Ws IAA2_{pro}:GUS lines were obtained from Dr Ranjan Swarup, University of
185 Nottingham and were grown on 50% MS pH 5.8 1% agar plates as described above, for 7 days
186 before AG2-1 inoculation. The plants were spaced at least 1 cm apart and 3 cm from the top of
187 the plate. Plates were inoculated using 6mm PDA plugs colonised with *R. solani* AG2-1. Three
188 plugs were used per plate, spaced equally, 2 cm from the bottom of the plate. The fungal growth
189 was close to, but not touching the roots, by 3 dpi. Samples were attempted at later time points

190 but after the fungus reached the plants, the roots were not able to be removed from the plates
191 and stained effectively without breaking.

192 GUS buffer was prepared with 100mM pH7.0 sodium phosphate buffer, 0.5M EDTA, 1mM
193 potassium ferricyanide, 1mM potassium ferrocyanide, 0.5% (w/v) 5-bromo-4-chloro-3-
194 indolyl- β -D-glucuronic acid (x-gluc; thermo scientific) dissolved in 1ml dimethylformamide
195 (DMX) and 0.1% (v/v) Triton x-100. Whole plants were harvested and immediately placed in
196 the prepared GUS buffer on ice until all samples were collected. Samples were incubated with
197 GUS buffer at 37°C for 30 minutes wrapped in foil. Samples were transferred to fresh tubes
198 with 25% ethanol overnight, before increasing the ethanol percentage over subsequent days
199 (50%, 70%, 90%, 100%), then the samples were stored in 50% glycerol until microscopy.
200 Samples were viewed using the Leica CTR5000 microscope (Leica Microsystems, Germany).

201 **Statistical Analysis**

202 Statistical analysis for all experiments were carried out using Genstat® Version 19 for windows
203 (VSN International Ltd, UK). Analysis of Variance (ANOVA) with t-test was conducted on
204 the data for the *B. napus* root and hypocotyl disease scores and on the proportional decrease of
205 root length due to inoculation. Student t-test was used to compare fold changes in gene
206 expression due to inoculation with AG2-1 for each OSR genotype at each timepoint. The
207 decrease in plant leaf areas of the *A. thaliana* mutants relative to their non-inoculated controls
208 were evaluated using student t-tests with differences considered significantly different at $P <$
209 0.05.

210 **Results**

211 Phenotypic comparison of *Brassica napus* varieties

212 Differences in the symptom severity between *B. napus* varieties inoculated with *R. solani* AG2-
213 1 were determined at 7 days post-inoculation (dpi) (Figure 1A, B). All varieties showed root
214 and hypocotyl symptoms and a reduction in root length under inoculation, but plants of cv.
215 Anastasia were most susceptible, showing extensive necrosis on both the root and hypocotyl
216 (root: 4/4, hypocotyl: 3.5/4) and total root length reduction by 95% under inoculation (Figure
217 1B, C). Campus showed the fewest symptoms on both the root and the hypocotyl and was
218 significantly more resistant to hypocotyl damping off than Saveo or Anastasia (Figure 1B).
219 Furthermore, Campus exhibited significantly lower reduction of root length due to inoculation,
220 compared to Anastasia (Figure 1C). Skye showed more severe symptoms than Campus but
221 grew the longest roots under inoculation, despite an 85% reduction in length (Supplementary
222 Figure 1 and Figure 1C). Symptom severity and root length reduction in Saveo and Sensia were
223 comparable to Anastasia and Skye, respectively (Figure 1B, C).

224 Anastasia, Skye, and Campus were chosen for further investigation using confocal microscopy
225 as these conventional genotypes represented contrasting disease severity phenotypes as shown
226 on Figure 1. Anastasia was identified as highly susceptible, Campus as most resistant and Skye
227 was intermediate due to some tolerance to disease since root growth was least inhibited despite
228 developing severe symptoms. Anastasia, Skye, and Campus roots were infected using *R. solani*
229 AG2-1 sclerotia and stained using Propidium Iodide and Alexa Fluor Wheat Germ Agglutinin
230 488 to visualise the infection (**Error! Reference source not found.**). Propidium iodide stains
231 plant cell walls, and the Alexa Fluor stains fungal hyphae. Hyphal networks forming from
232 germinated sclerotia and infection cushions were observed at 8, 24 and 48 hours post-
233 inoculation (hpi) on Anastasia (Figure 2). Sclerotia germination was observed on Skye at 8hpi
234 with smaller infection cushions, than observed on Anastasia, developing by 48hpi. Germination
235 from sclerotia was rarely seen at 8hpi on Campus, but some surface hyphal growth was

236 observed at 24 and 48hpi. There were no infection cushions observed in Campus at any time
237 point of the microscopic investigation carried out up to 48hpi.

238 Characterisation of defence and hormonal responses in *Brassica napus* and *Arabidopsis*
239 *thaliana*

240 RT-qPCRs were conducted using cDNA from whole plant RNA extractions with Log2 fold
241 changes of gene expression due to infection of Anastasia, Campus, and Skye shown at 8, 24
242 and 48hpi (Figures 3, 5, 7-10). AG2-1 reduces plant vigour, growth, and development of *A.*
243 *thaliana* (Supplementary Figure 2). To functionally confirm hormonal defence responses, *A.*
244 *thaliana* mutants were soil-inoculated with *R. solani* AG2-1 and assessed for disease effects on
245 plant growth above ground (Supplementary Figure 3), expressed as proportional reduction due
246 to inoculation before comparison to the wild type *A. thaliana* (WT, Col-0) (Figures 3, 5, 7-10).
247 Differential gene expression of OSR varieties for hormonal pathways and differences in
248 growth, due to inoculation, between WT and Arabidopsis mutants are described in relation to
249 the proposed defence diagram shown in Figure 11.

250 We first assessed the expression of AUX1 involved in auxin transport in plants, and AXR1 and
251 TIR1 as two major genes of auxin signalling. AUX1 was significantly upregulated in Anastasia
252 compared to Skye at 8 and 24hpi and declined in expression at 48hpi remaining significantly
253 less expressed in Skye compared to Campus (Figure 3A). AXR1 showed similar expression
254 pattern, although differences between varieties were not found to be statistically significant at
255 any time point (Figure 3B). TIR1 and the auxin-responsive gene IAA7 also had similar
256 expression patterns, with Anastasia upregulating both genes significantly more than Campus
257 at 24hpi (Figure 3C, D). The least auxin gene responsive variety at 24hpi was Campus,
258 followed at 48hpi by Skye with both showing repressed gene expression compared to Anastasia
259 (Figure 3C, D). These results showed that inoculation significantly increased the expression of

260 genes of auxin transport, signalling and response in the susceptible Anastasia compared to the
261 other two more tolerant genotypes. When gene functionality was tested in *A. thaliana* (Figure
262 3E), results showed that differences in above ground growth reduction of the mutants compared
263 to WT plants were small and not significant at $P < 0.05$. However, auxin signalling in the
264 susceptible WT *A. thaliana* roots increased by pathogen infection as *A. thaliana* IAA2_{pro}:GUS
265 lines showed more intense staining over the course of infection (Figure 4).

266 The basic-helix-loop-helix (bHLH) transcription factor, MYC2, differentially regulates
267 jasmonic acid (JA)-responsive defence to pests and pathogens (Kazan and Manners 2013). JA
268 is synthesised from α -linolenic acid and is converted to its bioactive form JA-Ile by JAR1
269 (Wang et al. 2021). JA-Ile promotes the ubiquitination and degradation of JAZ proteins via the
270 E3-ligase complex SCF-COI1. This causes the de-repression of MYC2 and ERF1, which form
271 two distinct, antagonistic signalling pathways (Kazan and Manners 2013). Inoculation
272 significantly upregulated JAR1 in Skye and Campus in contrast to Anastasia where gene
273 expression was repressed at 8hpi (Figure 5A). At 24hpi only Campus showed positive increase
274 in gene expression whilst a significant decrease was observed in Skye and Anastasia. At 48hpi,
275 Anastasia upregulated JAR1 significantly compared to Skye. MYC2 was highly expressed in
276 Anastasia at 24 and 48hpi compared to Campus and Skye (Figure 5B), suggesting that the
277 susceptible phenotype follows this branch of the JA signalling pathway. The *A. thaliana* mutant
278 *coil-4* showed a significantly greater reduction in growth under inoculation compared to the
279 WT (Figure 5C), supporting the role of JA-regulated defence response to *R. solani*. To visualise
280 JA response in the susceptible interaction, *A. thaliana* Jas9:VENUS lines were imaged under
281 inoculation with AG2-1 (**Error! Reference source not found.**) (Larrieu et al. 2015). In the
282 tissues near the root tip where *R. solani* had colonised, no fluorescence was observed,
283 indicating the complete degradation of JAZ9 proteins. However, in the susceptible WT root

284 tissues further away from the infection, JAZ9 appeared to be stabilised, indicating a reduction
285 in JA activity.

286 MYC2 is positively regulated by abscisic acid (ABA) (Kazan and Manners 2013). ABA is
287 synthesised from zeaxanthin, with the final two steps involving the conversion of xanthoxin by
288 a short chain alcohol dehydrogenase (ABA2) into abscisic aldehyde, and oxidation into ABA
289 by abscisic aldehyde oxidase (AAO3) (Finkelstein 2013). ABA can then form a complex with
290 ABA receptors (PYR/PYL/RCAR), which interact with PP2Cs, causing the de-repression of
291 SnRK2s and leading to the transcription of ABA-induced genes (Finkelstein 2013). AAO3 was
292 significantly downregulated in Anastasia compared to Skye at 8hpi, however by 48hpi
293 Anastasia significantly upregulated AAO3 compared to Campus or Skye (Figure 7A). ABI4 is
294 an ABA-regulated transcription factor, which has increased expression in the presence of ABA,
295 but is repressed by auxin (Saini et al. 2013). All varieties exhibited negative log₂ fold change
296 of ABI4 however Anastasia showed >15-fold repression at 8 and 24hpi compared to the other
297 two cultivars (Figure 7B). The *A. thaliana* mutants *aba2-1* and *abi4-1* showed similar
298 proportional reduction in growth due to inoculation and were as susceptible as the Col-0 to
299 AG2-1 (Figure 7C).

300 The transcription factor, ERF1, is negatively regulated by MYC2, but positively regulated by
301 ethylene (ET) synthesised from methionine (Wang et al. 2002). In high ET, EIN2 activates ET
302 signalling (Wang et al. 2002) with EIN3/EIL proteins promoting ERF1, which leads to
303 downstream ET-responsive transcription (Wang et al. 2002). ERF1 is a downstream
304 component of both ET and JA pathways, and can be activated by both independently, or
305 synergistically (Lorenzo et al. 2003). All varieties upregulated EIN2, however Anastasia
306 showed greater log₂ fold change of gene expression compared to Skye at 48hpi (Figure 8A).
307 There were no significant differences between varieties for ERF1 expression at 8 or 24hpi,
308 however at 48hpi, in response of infection, Campus and Skye increased ERF1 expression

309 significantly compared to Anastasia where expression was repressed 5-fold due to infection
310 (Figure 8B). PDF1.2, downstream of ERF1, showed significantly increased log₂ fold change
311 in expression in Skye at 8hpi, Skye and Campus at 24hpi, and just for Campus at 48hpi
312 compared to Anastasia or Skye (Figure 8C). These results indicated that the ERF1 pathway
313 contributes to defence against *R. Solani* AG2-1. The ET signalling mutant *Atein3eill* showed
314 a significant reduction in growth compared to WT *A. thaliana* (Figure 8D), suggesting that
315 plants with reduced ET- responsive transcription were highly susceptible to *R. solani* AG2-1
316 infection.

317 Mutually antagonistic crosstalk is known to exist between JA and salicylic acid (SA) and the
318 balance of action between these two hormones is particularly important in the host defence
319 responses to biotrophic and necrotrophic pathogens (Robert-Seilaniantz et al. 2011). SA is
320 synthesised via the ICS and PAL pathways (Lefevere et al. 2020). ICS1 (also known as SID2)
321 catalyses the first reaction of chorismate to isochorismate in the ICS pathway. PAL4 catalyses
322 the reaction of phenylalanine to trans-cinnamic acid (tCA) that can also lead to lignin
323 biosynthesis (Zheng et al. 2019; Lefevere et al. 2020). In response to inoculation at 8hpi and in
324 contrast to Campus, Anastasia downregulated both ICS1 and PAL4 (Figure 9A, B). ICS1 and
325 PAL4 expression increased by 20- and 10-fold, respectively at 24hpi in Anastasia compared to
326 the other two genotypes with higher expression maintained by Anastasia at 48hpi (Figure 9A,
327 B). High cytosolic SA leads to a redox change, causing cytosolic NPR1 oligomers to
328 monomerise and translocate to the nucleus. There, NPR1 enables the transcription of SA-
329 responsive genes enabling systemic acquired resistance (SAR) responses, and is then targeted
330 for degradation (Ding and Ding 2020). NPR1 is also required for induced systemic resistance
331 (ISR) independent of SA accumulation but requiring responsive JA or ET defence pathways
332 (Withers and Dong 2016). Anastasia and Campus upregulated NPR1 in response to infection
333 at 24 and 48hpi compared to Skye, in which gene expression was repressed (Figure 9C). The

334 final step of the biosynthesis of the phytoalexin, camalexin, derived from tryptophan, is
335 catalysed by PAD3 (Zhou et al. 1999; Schuhegger et al. 2006). In our studies, PAD3 expression
336 increased over time in Anastasia showing significantly higher log₂ fold change compared to
337 the other two varieties at 48hpi (Figure 9D). The *A. thaliana* mutants *sid2* and *npr1* showed
338 similar reduction in growth due to inoculation as the WT *A. thaliana* plants (Figure 9E).
339 However, the *A. thaliana pad3* mutant showed a significant reduction in growth under
340 inoculation compared to Col-0 suggesting that a reduction in camalexin biosynthesis increased
341 susceptibility to AG2-1.

342 NOXs known as respiratory burst oxidase homologs (RBOHs), mediate signal transduction
343 pathways via production of reactive oxygen species (ROS) and participate in the regulation of
344 plant development and growth processes, in addition to defence to biotic stress (Hu et al. 2020).
345 RBOHC, known as RHD2, is a key regulator of ROS accumulation in the roots involved in
346 root hair formation, and primary root elongation and development by regulating cell expansion
347 (Chapman et al. 2019; Hu et al. 2020). RBOHD is a membrane protein, which undergoes
348 conformational changes and phosphorylation during the influx of Ca²⁺ after pathogen
349 perception resulting in the production ROS (Lee et al. 2020). RBOHD can be directly
350 phosphorylated by DORN1 (Hu et al. 2020), which has been previously shown to enhance the
351 resistance of *A. thaliana* to *R. solani* AG8 (Kumar et al. 2020). RBOHC expression was
352 significantly higher in Anastasia compared to the other two genotypes at any time and
353 decreased over time (Figure 10A). Inoculation failed to affect the expression of RBOHC in
354 Skye or Campus. In contrast, RBOHD was significantly repressed in Anastasia at all time
355 points compared to the other two cultivars with Skye and Campus upregulating RBOHD at
356 48hpi (Figure 10B), supporting the hypothesis that RBOHD activity is involved in enhanced
357 resistance responses to AG2-1.

358 **Discussion**

359 To our knowledge, this is the first study to molecularly characterise the defence response of
360 OSR to its pathogen, *R. solani* AG2-1. The OSR varieties used here showed contrasting disease
361 phenotypes and defence pathways of their response to AG2-1. Using *A. thaliana* mutants, we
362 evaluated the functionality of key hormonal defence genes against *R. solani* AG2-1 to support
363 our gene expression studies. Our results showed that in contrast to auxin, JA and ET signalling
364 enhanced the resistance response to *R. solani* AG2-1.

365 Currently there are no *R. solani* AG2-1 resistant OSR varieties, however, we have shown that
366 some cultivar variation in susceptibility exists, with Anastasia being the most susceptible OSR
367 variety used in our studies, whilst Campus was the most resistant. These results were confirmed
368 using microscopy visualising the infection caused by sclerotia of *R. solani* on roots of *B. napus*.
369 We showed that infection cushions developed quickly and more abundantly on the more
370 susceptible host agreeing with previous research (Verma 1996) demonstrating that *R. solani*
371 hyphae penetrated rapidly in compatible interactions. Indeed, Anastasia exhibited severe root
372 rot and death quickly, whereas necrotic lesions formed slowly on the more resistant Campus
373 and Skye, with the latter two genotypes continuing to grow despite the infection suggesting
374 that seedling vigour and growth can be useful tolerance traits against the damping off effects
375 of AG2-1.

376 Molecular studies using RT-qPCRs showed different defence responses amongst the varieties,
377 which we supported with functional studies with Arabidopsis mutants. Our results showed a
378 strong link between increased auxin signalling and susceptibility to *R. solani* AG2-1. IAA is
379 synthesised from chorismate, via the tryptophan (Trp)-dependent or Trp-independent pathways
380 (Mano and Nemoto 2012) and functions through interactions with the E3-ligase complex SCF-
381 TIR1, which promotes the ubiquitination of AUX/IAA proteins and their subsequent

382 degradation (Sugawara et al. 2015). This leads to the de-repression of ARFs and the
383 transcription of auxin-responsive genes. LAX transporters, such as AUX1, are IAA influx
384 carriers, and are vital for IAA concentration gradients (Sugawara et al. 2015). The increased
385 auxin signalling in the susceptible hosts was demonstrated here with increased expression of
386 key auxin responsive genes and *A. thaliana* IAA2_{pro}:GUS lines supporting the hypothesis that
387 an auxin produced by the fungus is likely to be involved in the modification of host
388 development and defence. Indeed, previous work has identified a link between the production
389 of the auxin, phenyl acetic acid (PAA), by *R. solani* and its pathogenicity (Bartz et al. 2012).
390 The role of PAA in plants is less studied than IAA, but it is known to be synthesised from
391 phenylalanine, and is found at higher endogenous levels than IAA in various *A. thaliana* plant
392 tissues (Sugawara et al. 2015). In general, auxin-responsive genes can be regulated by both
393 IAA and PAA (Sugawara et al. 2015). It will thus be vital to uncover if *R. solani* AG2-1 is
394 producing PAA, and how this auxin and IAA produced by the fungus may be contributing to
395 the virulence of the pathogen, and to host susceptibility.

396 When plants are induced by exogenous auxin and the auxin–TIR–AUX/IAA–ARF signalling
397 is activated, JA synthesis is induced (Yang et al. 2019). JAR1 converts JA to JA-Ile with the
398 latter promoting the ubiquitination and degradation of JAZ proteins via the E3-ligase complex
399 SCF-COI1 (Wang et al. 2021) causing the release of MYC2 and ERF1, forming two distinct,
400 antagonistic signalling pathways (Kazan and Manners 2013). MYC2 plays a substantial role in
401 the crosstalk between growth and hormonal defence regulating pathways. For example, MYC2
402 is known to repress PLETHORA1 (PLT1) and PLT2 transcription factors, facilitating the
403 interaction between JA and auxin to inhibit root growth (Chen et al. 2011). This may have
404 contributed to the almost complete inhibition of root growth in inoculated Anastasia plants.
405 Furthermore, when using Jas9:VENUS lines under inoculation with AG2-1, we observed the
406 depletion of JA indicated by an increased Jas9:VENUS signal away from infection. Based on

407 the expression of the key genes of the JA signalling pathway and the functional analysis in
408 Arabidopsis, the MYC2 branch of the pathway was shown to contribute to increased
409 susceptibility to AG2-1.

410 The JAZs-MYC2 components play an important role in the crosstalk between JA and ABA
411 signalling pathways, affecting plant growth and defence (Chen et al. 2011). ABA enhances the
412 interaction between PYRABACTIN RESISTANCE1-Like protein (PYL6) and JAZ, activating
413 transcription of MYC2, which in turn activates the expression of the JA responsive gene VSP2
414 against herbivore damage, thus linking ABA and JA defence responses (Aleman et al. 2016).
415 However, this activity negatively regulates the ERF1/ORA59-PDF1.2 branch of the JA
416 pathway required for pathogen defence (Kazan and Manners 2013). The ABA biosynthesis
417 mutants (*aaos3* and *aba2*), as well as the ABA insensitive mutant (*abi4*) showed increased
418 susceptibility to the soil-borne oomycete *Pythium irregulare*, however, these mutants were
419 more resistant to the necrotroph *Botrytis cinerea* (Adie et al. 2007). We observed that *abi4-1*
420 and *aba2-1* showed similar susceptibility to the WT Arabidopsis however ABI4 expression
421 was downregulated >15-fold in the susceptible Anastasia under infection, compared to Campus
422 or Skye, suggesting that ABA signalling likely repressed by auxin (Saini et al. 2013) aided
423 susceptibility to *R. solani* AG2-1.

424 JAZs-MYC2 and EIN3/EIL1 of the JA and ET pathways, respectively, co-ordinate the plant
425 defence response against necrotrophic pathogens by activating the expression of the defence
426 protein PDF1.2 through ERF1 and ORA59 (Yang et al. 2019). ERF1 has previously been
427 shown to regulate resistance to many necrotrophic fungi including *B. cinerea*, *Plectosphaerella*
428 *cucumerina*, *Fusarium oxysporum* f. sp. *conglutinans* and *F. oxysporum* f. sp. *lycopersici*
429 (Berrocal-Lobo and Molina 2004). Similarly in our studies, the increased expression of ERF1
430 and PDF1.2 in Campus and Skye, in contrast to Anastasia, together with functional analysis
431 using *Atein3eill* supported our conclusion that the ET signalling pathway is a key regulator in

432 the host defence response to *R. solani* AG2-1. Molecular genetics approaches have shown
433 evidence that ET and NADPH oxidases act to co-ordinate plant responses to both abiotic and
434 biotic stress (Xia et al. 2015). In relation to biotic stress regulation, EIN2-mediated signalling
435 has been shown to be required for flagellin-induced RBOHD-dependent ROS accumulation
436 against bacterial pathogens (Xia et al. 2015). The *A. thaliana* double mutant *rbohfrboh* also
437 exhibits almost complete loss of resistance to *R. solani* AG8 (Foley et al. 2013). Taken together
438 with our results showing upregulation of RBOHD only in the more resistant Campus and Skye,
439 in contrast to repression in the susceptible Anastasia we suggest that ROS produced via
440 RBOHD is part of an effective defence response to *R. solani*. In contrast, RBOHC was
441 upregulated in Anastasia at all time points. The activity of RBOHC has been mostly associated
442 with regulation of root growth and development rather than the response to pathogenic attack
443 and its role in resistance or susceptibility to soil-borne pathogens is unknown. We can speculate
444 based on the expression of our contrasting varieties that RBOHC is not likely to be as effective
445 as RBOHD in the defence to AG2-1.

446 SA, synthesised via the ICS and PAL pathways, also plays a key role in ROS production
447 through the regulation of RBOH transcription, and can create a feedback loop where ROS also
448 regulate SA signalling (Lukan and Coll 2022). In our studies ICS1 and PAL4 were upregulated
449 significantly more in Anastasia than in Campus or Skye and although the *A. thaliana* mutant
450 *sid2* showed similar susceptibility as the WT plants to the disease these results together suggest
451 that SA biosynthesis is likely to contribute to susceptibility. Previously OsPAL4 was identified
452 as contributing to resistance to *R. solani* AG2 (Tonnessen et al. 2015) and BnPAL4 activity
453 was increased in resistant OSR during *Verticillium longisporum* infection (Zheng et al. 2019).
454 The role of PAL4 in secondary metabolism in the interaction with AG2-1 requires further
455 investigation as we observed increased expression in the most resistant variety, Campus,
456 compared to the tolerant Skye. The importance of NPR1 for the response to *R. solani* or other

457 soil-borne pathogens including *P. irregulare* (Adie et al. 2007) has been demonstrated in
458 various reports. For example, tissue-specific expression of AtNPR1 in rice has been shown in
459 previous research to confer resistance to *R. solani* AG1-1A (Molla et al. 2016). Similarly
460 expression of BjNPR1 in mungbean also increased resistance to *R. solani* (AG not specified)
461 (Vijayan and Kirti 2012). However, here differences in NPR1 expression of OSR varieties and
462 the growth phenotype of the *A. thaliana npr1* mutant under inoculation suggested that NPR1
463 may play a dual role in the disease response depending on the simultaneous activity of other
464 hormones. Thus, the increased expression of NPR1 in the susceptible Anastasia was associated
465 with NPR1 enabled transcription of SA-responsive genes for SAR (Ding and Ding 2020) in
466 contrast to Campus, where NPR1 functionality was required for ISR that is independent of SA
467 accumulation, but dependant on responsive JA/ET defence pathways (Withers and Dong 2016).
468 PAD3 encodes the cytochrome P450 enzyme CYP71B15 that catalyses the last step of
469 camalexin biosynthesis, and camalexin plays an important role in both SAR and ISR (Nguyen
470 et al. 2022). SA, but not JA or ET, has been shown to be required for ISR associated with
471 camalexin accumulation. Whilst *Atpad3* mutants were susceptible to *R. solani* suggesting a link
472 between camalexin production and defence, greater PAD3 activity was observed in the
473 susceptible Anastasia. Whilst contradicting, these results are in part explained by the ability of
474 *R. solani* AG2-1 to effectively detoxify camalexin (Pedras and Liu 2004), suggesting an
475 advantageous pathogen adaptation strategy where SAR or ISR involving camalexin are
476 rendered ineffective against AG2-1.

477 In conclusion, our investigations have shown that susceptibility responses to *R. solani* AG2-1
478 vary among commercially available varieties of *B. napus*. Cv. Anastasia was most susceptible,
479 Campus showed fewest symptoms, while Skye showed a degree of tolerance under inoculation.
480 Investigating the relative expression of known defence pathway genes in the *B. napus* varieties,
481 mutants and transgenic lines in *A. thaliana* has suggested that auxin signalling plays a role in

482 susceptibility to AG2-1 of *R. solani*. ABA signalling, likely modified by auxin in compatible
 483 interactions, and the MYC2 component of JA signalling were also associated with
 484 susceptibility (Figure 11). In contrast, increased defence response was driven by JA/ET
 485 signalling and RBOHD (Figure 11). Further studies examining the genetic differences between
 486 the OSR varieties used here can identify genes or markers that will inform breeding programs,
 487 and lead to the development of more resilient OSR varieties. The broad host range of *R. solani*
 488 AG2-1 makes this research findings important for other crops within the same family such as
 489 vegetable Brassicas. With limited chemical control options available, it is vital that *R. solani*
 490 resistant crops are developed to maintain future yields in fields with high inoculum.

491 **Acknowledgements**

492 Isabelle L. Sims was funded by BBSRC via the University of Nottingham Biotechnology and
 493 Biological Sciences Doctoral Training Programme.

494 **References**

- 495 Adie, B.A.T., Pérez-Pérez, J., Pérez-Pérez, M.M., Godoy, M., Sánchez-Serrano, J.J.,
 496 Schmelz, E.A. and Solano, R., 2007. ABA is an essential signal for plant resistance to
 497 pathogens affecting JA biosynthesis and the activation of defenses in Arabidopsis. *Plant*
 498 *Cell* [Online], 19(5), pp.1665–1681. Available from:
 499 <https://doi.org/10.1105/tpc.106.048041>.
- 500 Ajigboye, O.O., Jayaweera, D.P., Angelopoulou, D., Ruban, A. V., Murchie, E.H., Pastor, V.,
 501 Summers, R. and Ray, R. V., 2021. The role of photoprotection in defence of two wheat
 502 genotypes against *Zymoseptoria tritici*. *Plant Pathology* [Online], 70(6), pp.1421–1435.
 503 Available from: <https://doi.org/10.1111/ppa.13392>.
- 504 Aleman, F., Yazaki, J., Lee, M., Takahashi, Y., Kim, A.Y., Li, Z., Kinoshita, T., Ecker, J.R.
 505 and Schroeder, J.I., 2016. An ABA-increased interaction of the PYL6 ABA receptor
 506 with MYC2 Transcription Factor: A putative link of ABA and JA signaling. *Scientific*
 507 *Reports* [Online], 6(June), pp.1–7. Available from: <https://doi.org/10.1038/srep28941>.
- 508 Bartz, F.E., Glassbrook, N.J., Danehower, D.A. and Cubeta, M.A., 2012. Elucidating the role
 509 of the phenylacetic acid metabolic complex in the pathogenic activity of *Rhizoctonia*
 510 *solani* anastomosis group 3. *Mycologia* [Online], 104(4), pp.793–803. Available from:
 511 <https://doi.org/10.3852/11-084>.
- 512 Berrocal-Lobo, M. and Molina, A., 2004. Ethylene Response Factor 1 Mediates Arabidopsis
 513 Resistance to the Soilborne Fungus *Fusarium oxysporum*. *Molecular Plant-Microbe*

- 514 *Interactions* [Online], 17(7), pp.763–770. Available from:
515 <https://doi.org/10.1094/mpmi.2004.17.7.763>.
- 516 Brown, M., Jayaweera, D.P., Hunt, A., Woodhall, J.W., and Ray, R.V. 2021. Yield Losses
517 and Control by Sedaxane and Fludioxonil of Soilborne Rhizoctonia, Microdochium, and
518 Fusarium Species in Winter Wheat. *Plant disease* [Online] 105, pp.2521-2530.
519 Available from: <https://doi.org/10.1094/PDIS-11-20-2401-RE>
- 520 Carling, D.E., Kuninaga, S. and Brainard, K.A., 2002. Hyphal anastomosis reactions, rDNA-
521 internal transcribed spacer sequences, and virulence levels among subsets of
522 *Rhizoctonia solani* anastomosis group-2 (AG-2) and AG-BI. *Phytopathology* [Online],
523 92(1), pp.43–50. Available from: <https://doi.org/10.1094/PHTO.2002.92.1.43>.
- 524 Chapman, J.M., Muhlemann, J.K., Gayomba, S.R. and Muday, G.K., 2019. RBOH-
525 Dependent ROS Synthesis and ROS Scavenging by Plant Specialized Metabolites to
526 Modulate Plant Development and Stress Responses. *Chemical Research in Toxicology*
527 [Online], 32(3), pp.370–396. Available from:
528 <https://doi.org/10.1021/acs.chemrestox.9b00028>.
- 529 Chen, Q., Sun, J., Zhai, Q., Zhou, W., Qi, L., Xu, L., Wang, B., Chen, R., Jiang, H., Qi, X.,
530 Palme, K. and Li, C., 2011. The Basic Helix-Loop-Helix Transcription Factor MYC2
531 Directly Represses PLETHORA Expression during Jasmonate-Mediated Modulation of
532 the Root Stem Cell Niche in Arabidopsis. *The Plant Cell*, 23, pp.3335–3352.
- 533 Cordovez, V., Mommer, L., Moisan, K., Lucas-Barbosa, D., Pierik, R., Mumm, R., Carrion,
534 V.J. and Raaijmakers, J.M., 2017. Plant phenotypic and transcriptional changes induced
535 by volatiles from the fungal root pathogen *Rhizoctonia solani*. *Frontiers in Plant*
536 *Science* [Online], 8(July), pp.1–14. Available from:
537 <https://doi.org/10.3389/fpls.2017.01262>.
- 538 Ding, P. and Ding, Y., 2020. Stories of Salicylic Acid: A Plant Defense Hormone. *Trends in*
539 *Plant Science* [Online], 25(6), pp.549–565. Available from:
540 <https://doi.org/10.1016/j.tplants.2020.01.004>.
- 541 Drizou, F., Graham, N.S., Bruce, T.J.A. and Ray, R. V., 2017. Development of high-
542 throughput methods to screen disease caused by *Rhizoctonia solani* AG 2-1 in oilseed
543 rape. *Plant Methods* [Online], 13(1), pp.1–14. Available from:
544 <https://doi.org/10.1186/s13007-017-0195-1>.
- 545 Finkelstein, R., 2013. Abscisic Acid Synthesis and Response. *The Arabidopsis Book*
546 [Online], 11, p.e0166. Available from: <https://doi.org/10.1199/tab.0166>.
- 547 Foley, R.C., Gleason, C.A., Anderson, J.P., Hamann, T. and Singh, K.B., 2013. Genetic and
548 Genomic Analysis of *Rhizoctonia solani* Interactions with Arabidopsis; Evidence of
549 Resistance Mediated through NADPH Oxidases. *PLoS ONE* [Online], 8(2). Available
550 from: <https://doi.org/10.1371/journal.pone.0056814>.
- 551 Furukawa, T., Syono, K. 1998. Increased Production of IAA by *Rhizoctonia solani* is Induced
552 by Culture Filtrate from Rice Suspension Cultures, *Plant Cell Physiol* [Online], 39 (1),
553 pp.43–48, Available from: <https://doi.org/10.1093/oxfordjournals.pcp.a029287>
- 554 Hu, C.H., Wang, P.Q., Zhang, P.P., Nie, X.M., Li, B. Bin, Tai, L., Liu, W.T., Li, W.Q. and
555 Chen, K.M., 2020. NADPH Oxidases: The Vital Performers and Center Hubs during
556 Plant Growth and Signaling. *Cells* [Online], 9(2), pp.1–41. Available from:
557 <https://doi.org/10.3390/cells9020437>.
- 558 Iacobellis, N.S. and DeVay, J.E., 1987. Studies on pathogenesis of *Rhizoctonia solani* in

- 559 beans: an evaluation of the possible roles of phenylacetic acid and its hydroxy
560 derivatives as phytotoxins. *Physiological and Molecular Plant Pathology* [Online],
561 30(3), pp.421–432. Available from: [https://doi.org/10.1016/0885-5765\(87\)90021-X](https://doi.org/10.1016/0885-5765(87)90021-X).
- 562 Jayaweera, D., and Ray, R.V. 2022. Yield loss and integrated disease control of *Rhizoctonia*
563 *solani* AG2-1 using seed treatment and sowing rate of oilseed rape. *Plant disease*
564 [Online] First look, Available from: <https://doi.org/10.1094/PDIS-08-22-1817-RE>
- 565 Kataria, H.R. and Verma, P.R., 1992. *Rhizoctonia solani* damping-off and root rot in oilseed
566 rape and canola. *Crop Protection* [Online], 11(1), pp.8–13. Available from:
567 [https://doi.org/10.1016/0261-2194\(92\)90072-D](https://doi.org/10.1016/0261-2194(92)90072-D).
- 568 Kazan, K. and Manners, J.M., 2013. MYC2: The master in action. *Molecular Plant* [Online],
569 6(3), pp.686–703. Available from: <https://doi.org/10.1093/mp/sss128>.
- 570 Kidd, B.N., Foley, R., Singh, K.B. and Anderson, J.P., 2021. Foliar resistance to *Rhizoctonia*
571 *solani* in *Arabidopsis* is compromised by simultaneous loss of ethylene, jasmonate and
572 PEN2 mediated defense pathways. *Scientific Reports* [Online], 11(1), pp.1–14.
573 Available from: <https://doi.org/10.1038/s41598-021-81858-5>.
- 574 Kumar, S., Tripathi, D., Okubara, P.A. and Tanaka, K., 2020. Purinoceptor P2K1/DORN1
575 Enhances Plant Resistance Against a Soilborne Fungal Pathogen, *Rhizoctonia solani*.
576 *Frontiers in Plant Science* [Online], 11(September), pp.1–10. Available from:
577 <https://doi.org/10.3389/fpls.2020.572920>.
- 578 Lakshman, D.K., Liu, C., Mishra, P.K. and Tavantzis, S., 2006. Characterization of the *arom*
579 gene in *Rhizoctonia solani*, and transcription patterns under stable and induced
580 hypovirulence conditions. *Current Genetics* [Online], 49(3), pp.166–177. Available
581 from: <https://doi.org/10.1007/s00294-005-0005-6>.
- 582 Larrieu, A., Champion, A., Legrand, J., Lavenus, J., Mast, D., Brunoud, G., Oh, J.,
583 Guyomarc'H, S., Pizot, M., Farmer, E.E., Turnbull, C., Vernoux, T., Bennett, M.J. and
584 Laplaze, L., 2015. A fluorescent hormone biosensor reveals the dynamics of jasmonate
585 signalling in plants. *Nature Communications* [Online], 6(May 2014), pp.1–9. Available
586 from: <https://doi.org/10.1038/ncomms7043>.
- 587 Lee, D.H., Lal, N.K., Lin, Z.J.D., Ma, S., Liu, J., Castro, B., Toruño, T., Dinesh-Kumar, S.P.
588 and Coaker, G., 2020. Regulation of reactive oxygen species during plant immunity
589 through phosphorylation and ubiquitination of RBOHD. *Nature communications*
590 [Online], 11(1), p.1838. Available from: <https://doi.org/10.1038/s41467-020-15601-5>.
- 591 Lefevre, H., Bauters, L. and Gheysen, G., 2020. Salicylic Acid Biosynthesis in Plants.
592 *Frontiers in Plant Science* [Online], 11(April), pp.1–7. Available from:
593 <https://doi.org/10.3389/fpls.2020.00338>.
- 594 Livak, K.J. and Schmittgen, T.D., 2001. Analysis of relative gene expression data using real-
595 time quantitative PCR and the 2- $\Delta\Delta$ CT method. *Methods* [Online], 25(4), pp.402–408.
596 Available from: <https://doi.org/10.1006/meth.2001.1262>.
- 597 Lobet, G., Pagès, L. and Draye, X., 2011. A novel image-analysis toolbox enabling
598 quantitative analysis of root system architecture. *Plant Physiology* [Online], 157(1),
599 pp.29–39. Available from: <https://doi.org/10.1104/pp.111.179895>.
- 600 Lorenzo, O., Piqueras, R., Sánchez-serrano, J.J. and Solano, R., 2003. ETHYLENE
601 RESPONSE FACTOR1 integrates signals from Ethylene and Jasmonate pathways in
602 plant defense. [Online], 15, pp.165–178. Available from:
603 <https://doi.org/10.1105/tpc.007468.signaling>.

- 604 Lukan, T. and Coll, A., 2022. Intertwined Roles of Reactive Oxygen Species and Salicylic
605 Acid Signaling Are Crucial for the Plant Response to Biotic Stress. *International*
606 *Journal of Molecular Sciences* [Online], 23(10). Available from:
607 <https://doi.org/10.3390/ijms23105568>.
- 608 Mandava, N.B., Orellana, R.G., David Warthen, J., Worley, J.F., Dutky, S.R., Finegold, H.
609 and Weathington, B.C., 1980. Phytotoxins in *Rhizoctonia Solani*: Isolation and
610 Biological Activity of m-Hydroxy-and m-Methoxyphenylacetic Acids. *Journal of*
611 *Agricultural and Food Chemistry* [Online], 28(1), pp.71–75. Available from:
612 <https://doi.org/10.1021/jf60227a009>.
- 613 Mano, Y. and Nemoto, K., 2012. The pathway of auxin biosynthesis in plants. *Journal of*
614 *Experimental Botany* [Online], 63(8), pp.2853–2872. Available from:
615 <https://doi.org/10.1093/jxb/ers091>.
- 616 Molla, K.A., Karmakar, S., Chanda, P.K., Sarkar, S.N., Datta, S.K. and Datta, K., 2016.
617 Tissue-specific expression of Arabidopsis NPR1 gene in rice for sheath blight resistance
618 without compromising phenotypic cost. *Plant Science* [Online], 250, pp.105–114.
619 Available from: <https://doi.org/10.1016/j.plantsci.2016.06.005>.
- 620 Nguyen, N.H., Trotel-Aziz, P., Villaume, S., Rabenoelina, F., Clément, C., Baillieul, F. and
621 Aziz, A., 2022. Priming of camalexin accumulation in induced systemic resistance by
622 beneficial bacteria against *Botrytis cinerea* and *Pseudomonas syringae* pv. tomato
623 DC3000 . *Journal of Experimental Botany* [Online], 73(11), pp.3743–3757. Available
624 from: <https://doi.org/10.1093/jxb/erac070>.
- 625 Pedras, M.S.C. and Liu, J., 2004. Designer phytoalexins : probing camalexin detoxi fi cation
626 pathways in the phytopathogen *Rhizoctonia solani* †. pp.1–7.
- 627 Redkar, A., Jaeger, E. and Doehlemann, G., 2018. Visualization of Growth and Morphology
628 of Fungal Hyphae in planta Using WGA-AF488 and Propidium Iodide Co-staining. *Bio-*
629 *Protocol* [Online], 8(14), pp.1–7. Available from:
630 <https://doi.org/10.21769/bioprotoc.2942>.
- 631 Robert-Seilaniantz, A., Grant, M. and Jones, J.D.G., 2011. Hormone crosstalk in plant
632 disease and defense: More than just JASMONATE-SALICYLATE antagonism. *Annual*
633 *Review of Phytopathology* [Online], 49, pp.317–343. Available from:
634 <https://doi.org/10.1146/annurev-phyto-073009-114447>.
- 635 Saini, S., Sharma, I., Kaur, N. and Pati, P.K., 2013. Auxin: A master regulator in plant root
636 development. *Plant Cell Reports* [Online], 32(6), pp.741–757. Available from:
637 <https://doi.org/10.1007/s00299-013-1430-5>.
- 638 Schmittgen, T., Livak, K. 2008. Analyzing real-time PCR data by the comparative CT
639 method. *Nat Protoc* [Online], 3, pp.1101–1108. Available from:
640 <https://doi.org/10.1038/nprot.2008.73>
- 641 Schneider, C.A., Rasband, W.S. and Eliceiri, K.W., 2012. NIH Image to ImageJ: 25 years of
642 Image Analysis. *Nat Methods* [Online], 9(7), pp.671–675. Available from:
643 https://doi.org/10.1007/978-1-84882-087-6_9.
- 644 Schuegger, R., Nafisi, M., Mansourova, M., Petersen, B.L., Olsen, C.E., Svatoš, A., Halkier,
645 B.A. and Glawischnig, E., 2006. CYP71B15 (PAD3) catalyzes the final step in
646 camalexin biosynthesis. *Plant Physiology* [Online], 141(4), pp.1248–1254. Available
647 from: <https://doi.org/10.1104/pp.106.082024>.
- 648 Sharon, M., Freeman, S. and Sneh, B., 2011. Assessment of resistance pathways induced in

- 649 Arabidopsis thaliana by hypovirulent Rhizoctonia spp. isolates. *Phytopathology*
650 [Online], 101(7), pp.828–838. Available from: [https://doi.org/10.1094/phyto-09-10-](https://doi.org/10.1094/phyto-09-10-0247)
651 0247.
- 652 Sugawara, S., Mashiguchi, K., Tanaka, K., Hishiyama, S., Sakai, T., Hanada, K., Kinoshita-
653 Tsujimura, K., Yu, H., Dai, X., Takebayashi, Y., Takeda-Kamiya, N., Kakimoto, T.,
654 Kawaide, H., Natsume, M., Estelle, M., Zhao, Y., Hayashi, K.I., Kamiya, Y. and
655 Kasahara, H., 2015. Distinct characteristics of indole-3-acetic acid and phenylacetic
656 acid, two common auxins in plants. *Plant and Cell Physiology* [Online], 56(8), pp.1641–
657 1654. Available from: <https://doi.org/10.1093/pcp/pcv088>.
- 658 Tonnessen, B.W., Manosalva, P., Lang, J.M., Baraoidan, M., Bordeos, A., Mauleon, R.,
659 Oard, J., Hulbert, S., Leung, H. and Leach, J.E., 2015. Rice phenylalanine ammonia-
660 lyase gene OsPAL4 is associated with broad spectrum disease resistance. *Plant*
661 *Molecular Biology* [Online], 87(3), pp.273–286. Available from:
662 <https://doi.org/10.1007/s11103-014-0275-9>.
- 663 Verma, P.R., 1996. Biology and control of Rhizoctonia solani on rapeseed : A review.
664 *Phytoprotection* [Online], 77(3), pp.99–111. Available from:
665 <https://doi.org/10.7202/706106ar>.
- 666 Vijayan, S. and Kirti, P.B., 2012. Mungbean plants expressing BjNPR1 exhibit enhanced
667 resistance against the seedling rot pathogen, Rhizoctonia solani. *Transgenic Research*
668 [Online], 21(1), pp.193–200. Available from: [https://doi.org/10.1007/s11248-011-9521-](https://doi.org/10.1007/s11248-011-9521-y)
669 y.
- 670 VSN International, 2019. GenStat for Windows 20th Edition [Online]. Hemel Hempstead,
671 UK. Available from: Genstat.co.uk.
- 672 Wang, K.L.C., Li, H. and Ecker, J.R., 2002. Ethylene biosynthesis and signaling networks.
673 *Plant Cell* [Online], 14(SUPPL.), pp.131–152. Available from:
674 <https://doi.org/10.1105/tpc.001768>.
- 675 Wang, Y., Mostafa, S., Zeng, W. and Jin, B., 2021. Function and Mechanism of Jasmonic
676 Acid in Plant Responses to Abiotic and Biotic Stresses. *International Journal of*
677 *Molecular Sciences* [Online], 22(8568). Available from: [https://doi.org/https://doi.org/](https://doi.org/https://doi.org/10.3390/ijms22168568)
678 10.3390/ijms22168568.
- 679 Withers, J. and Dong, X., 2016. Posttranslational Modifications of NPR1: A Single Protein
680 Playing Multiple Roles in Plant Immunity and Physiology. *PLoS Pathogens* [Online],
681 12(8), pp.1–9. Available from: <https://doi.org/10.1371/journal.ppat.1005707>.
- 682 Xia, X.J., Zhou, Y.H., Shi, K., Zhou, J., Foyer, C.H. and Yu, J.Q., 2015. Interplay between
683 reactive oxygen species and hormones in the control of plant development and stress
684 tolerance. *Journal of Experimental Botany* [Online], 66(10), pp.2839–2856. Available
685 from: <https://doi.org/10.1093/jxb/erv089>.
- 686 Yang, J., Duan, G., Li, C., Liu, L., Han, G., Zhang, Y. and Wang, C., 2019. The Crosstalks
687 Between Jasmonic Acid and Other Plant Hormone Signaling Highlight the Involvement
688 of Jasmonic Acid as a Core Component in Plant Response to Biotic and Abiotic
689 Stresses. *Frontiers in Plant Science* [Online], 10. Available from:
690 <https://doi.org/10.3389/fpls.2019.01349>.
- 691 Zheng, X., Koopmann, B. and von Tiedemann, A., 2019. Role of salicylic acid and
692 components of the phenylpropanoid pathway in basal and cultivar-related resistance of
693 oilseed rape (Brassica napus) to Verticillium longisporum. *Plants* [Online], 8(11).

694 Available from: <https://doi.org/10.3390/plants8110491>.

695 Zhou, N., Tootle, T.L. and Glazebrook, J., 1999. Arabidopsis PAD3, a gene required for
696 camalexin biosynthesis, encodes a putative cytochrome P450 monooxygenase. *Plant*
697 *Cell* [Online], 11(12), pp.2419–2428. Available from:
698 <https://doi.org/10.1105/tpc.11.12.2419>.

699

700 **Figure Legends**

701 Figure 1. *Brassica napus* disease symptom scores and damping off effects on root length at 7
702 days post inoculation with *Rhizoctonia solani* AG2-1. A) Plants were scored from 0-4; 0:
703 symptomless, 1: 25% symptoms, 2: 50% symptoms, 3: 75% symptoms, 4: death. B) Average
704 disease symptom scores for five commercially available *B. napus* varieties. Dark grey bars
705 show average hypocotyl symptom scores and light grey bars show average root symptom
706 scores. Non-inoculated data not shown as no individuals showed symptoms. C) Proportional
707 reduction in root length (relative to non-inoculated plant roots) due to AG2-1 measured using
708 ImageJ and SmartRoot plugin. The total length includes lateral roots. Error bars indicate
709 standard error (SE). Different letters above the bars indicated significant differences using t-
710 test, $p < 0.05$.

711 Figure 2. Confocal microscopy images showing *Rhizoctonia solani* AG2-1 sclerotia infection
712 on different *Brassica napus* varieties up to 2 days post-inoculation. Alexa Fluor Wheat Germ
713 Agglutinin 488 and Propidium Iodide staining of fungal tissues and *B. napus* roots,
714 respectively, showing the development of infection structures in Anastasia, Skye, and Campus.
715 Yellow arrowheads indicate infection cushions. Red shows staining with Alexa Fluor Wheat
716 Germ Agglutinin 488. Blue shows staining with Propidium Iodide. The images shown were
717 chosen as representatives from a minimum of nine samples of infected roots for each variety.
718 Scale bar = 250 μ m.

719 Figure 3. Effect of *Rhizoctonia solani* AG2-1 inoculation on auxin transport and signalling
720 genes (A) AUX1, (B) AXR1, (C) TIR1 and (D) IAA7 in *Brassica napus* varieties Anastasia,
721 Skye and Campus at 8, 24 and 48 hours post inoculation, and (E) proportional reduction in
722 plant leaf area (relative to non-inoculated plants) of *Arabidopsis thaliana* mutant plants at 11
723 days post inoculation with *Rhizoctonia solani* AG2-1. The data represent log₂ fold change of
724 differential gene expression using non-inoculated plants as internal calibrant. Error bars
725 indicate standard error (SE). Asterisk indicates a significant difference according to Student t
726 test, $p < 0.05$.

727 Figure 4. Response of *Arabidopsis thaliana* IAA_{pro}:GUS lines to *Rhizoctonia solani* AG2-1
728 at 1 and 3 days post-inoculation. Light microscopy images showing GUS staining in Ws
729 IAA_{pro}:GUS plants. At the time of sampling, *R. solani* growth had not reached the root of
730 plants. Scale bar = 100µm.

731 Figure 5. Effect of *Rhizoctonia solani* AG2-1 inoculation on Jasmonic acid signalling genes
732 (A) JAR1 and (B) MYC2 in *Brassica napus* varieties Anastasia, Skye and Campus at 8, 24 and
733 48 hours post inoculation, and (C) proportional reduction in plant leaf area (relative to non-
734 inoculated plants) of *Arabidopsis thaliana* mutant plants at 11 days post inoculation with
735 *Rhizoctonia solani* AG2-1. The data represent log₂ fold change of differential gene expression
736 using non-inoculated plants as internal calibrant. Error bars indicate standard error (SE).
737 Asterisk indicates a significant difference according to Student t test, $p < 0.05$.

738 Figure 6. Confocal microscopy images of *Arabidopsis thaliana* Jas9:VENUS seedlings
739 showing Jasmonic acid response to *R. solani* AG2-1 inoculation. Images are ordered left to
740 right reflecting their location within the taproot relative to the root tip, i.e. Farther right is the
741 root tip, and left is furthest from the root tip. Fluorescence from the Jas9:VENUS biosensor is
742 shown in green. Scale bar = 100µm.

743 Figure 7. Effect of *Rhizoctonia solani* AG2-1 inoculation on Abscisic acid biosynthesis genes
744 (A) AAO3 and (B) ABI4 in *Brassica napus* varieties Anastasia, Skye and Campus at 8, 24 and
745 48 hours post inoculation, and (C) proportional reduction in plant leaf area (relative to non-
746 inoculated plants) of *Arabidopsis thaliana* mutant plants at 11 days post inoculation with *R.*
747 *solani* AG2-1. The data represent log₂ fold change of differential gene expression using non-
748 inoculated plants as internal calibrant. Error bars indicate standard error (SE). Asterisk
749 indicates a significant difference according to Student t test, $p < 0.05$.

750 Figure 8. Effect of *Rhizoctonia solani* AG2-1 inoculation on Ethylene signalling genes (A)
751 EIN2, (B) ERF1 and (C) PDF1.2 in *Brassica napus* varieties Anastasia, Skye and Campus at
752 8, 24 and 48 hours post inoculation, and (D) proportional reduction in plant leaf area (relative
753 to non-inoculated plants) of *Arabidopsis thaliana* mutant plants at 11 days post inoculation
754 with *R. solani* AG2-1. The data represent log₂ fold change of differential gene expression using
755 non-inoculated plants as internal calibrant. Error bars indicate standard error (SE). Asterisk
756 indicates a significant difference according to Student's t test, $p < 0.05$.

757 Figure 9. Effect of *Rhizoctonia solani* AG2-1 inoculation on Salicylic acid signalling genes (A)
758 ICS1, (B) PAL4, (C) NPR1 and (D) PAD3 in *Brassica napus* varieties Anastasia, Skye and
759 Campus at 8, 24 and 48 hours post inoculation, and (E) proportional reduction in plant leaf area
760 (relative to non-inoculated plants) of *Arabidopsis thaliana* mutant plants at 11 days post
761 inoculation with *R. solani* AG2-1. The data represent log₂ fold change of differential gene
762 expression using non-inoculated plants as internal calibrant. Error bars indicate standard error
763 (SE). Asterisk indicates a significant difference according to Student's t test, $p < 0.05$.

764 Figure 10. Effect of *Rhizoctonia solani* AG2-1 inoculation on respiratory burst oxidase
765 homologs (RBOHs) genes mediating signal transduction via reactive oxygen species
766 production (A) RBOHC and (B) RBOHD in *Brassica napus* varieties Anastasia, Skye and

767 Campus at 8, 24 and 48 hours post inoculation. The data represent log₂ fold change of
768 differential gene expression using non-inoculated plants as internal calibrant. Error bars
769 indicate standard error (SE). Asterisk indicates a significant difference according to Student t
770 test, $p < 0.05$.

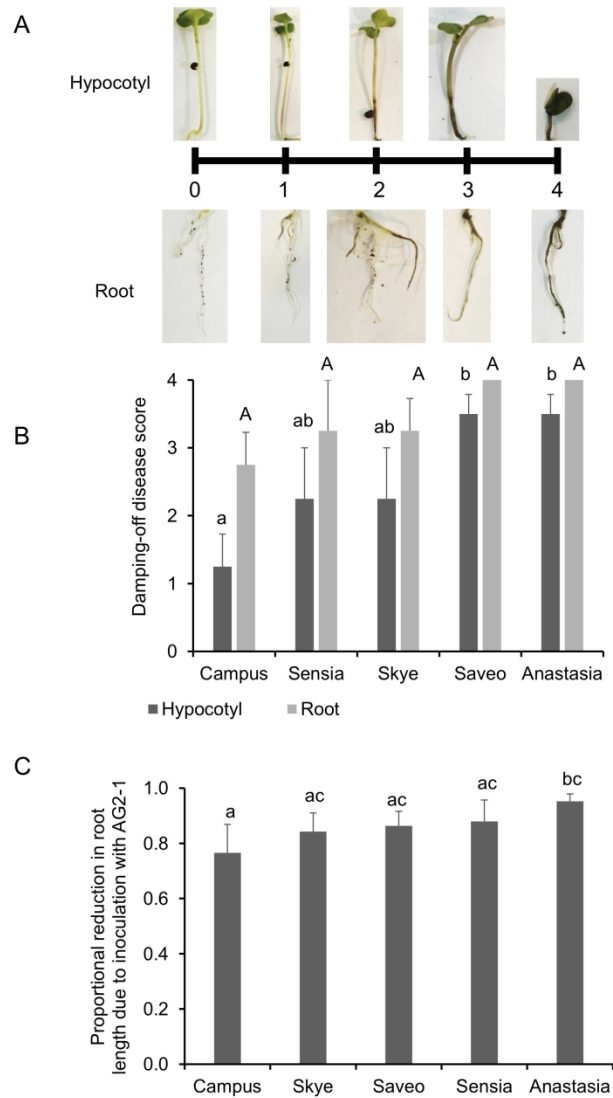
771 Figure 11. Proposed diagram of hormonal defence pathways involved in the Brassica-
772 *Rhizoctonia solani* AG2-1 interaction. Underlined genes have been tested in this work. Auxin
773 signalling and abscisic acid (ABA) signalling, with the latter likely modified by auxin in
774 compatible interactions, and the MYC2 component of jasmonic acid (JA) signalling together
775 with RBOHC were associated with susceptibility of Brassica hosts to AG2-1 of *R. solani*. In
776 contrast, JA/ethylene (ET) signalling and RBOHD enhanced the defence response to the
777 pathogen. NPR1 functionality dependant on responsive JA/ET defence pathways contributed
778 to induced systemic resistance (ISR) and enhanced defence to AG2-1. In contrast, SAR or ISR
779 by salicylic acid and PAD3 activity were associated with susceptible responses.

780 Supplementary Figure 1. Effect of *Rhizoctonia solani* AG2-1 inoculation on root length (cm)
781 of cvs. Campus, Skye, Saveo, Sensia and Anastasia of *Brassica napus* (oilseed rape). Error
782 bars indicate standard error (SE). Asterisk indicates a significant difference according to
783 Student's t test, $p < 0.05$.

784 Supplementary Figure 2. Effect of *Rhizoctonia solani* AG2-1 inoculation on (A) plant leaf area
785 of *Arabidopsis thaliana* (Col-0). Images (B) of inoculated and healthy plants shown at 11 days
786 post inoculation. Error bars indicate standard error (SE). Asterisk indicates a significant
787 difference according to Student's t test, $p < 0.05$. Scale bar = 1 cm.

788 Supplementary Figure 3. Effect of *Rhizoctonia solani* AG2-1 inoculation on plant leaf area of
789 Columbia-0 (Col-0) and mutants of *Arabidopsis thaliana* at 11 days post inoculation. Error

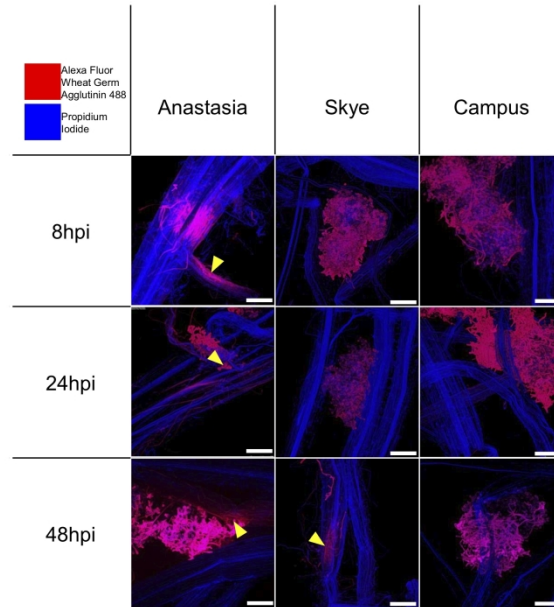
790 bars indicate standard error (SE). Asterisk indicates a significant difference according to
791 Student's t test, $p < 0.05$.



Brassica napus disease symptom scores and damping off effects on root length at 7 days post inoculation with *Rhizoctonia solani* AG2-1. A) Plants were scored from 0-4; 0: symptomless, 1: 25% symptoms, 2: 50% symptoms, 3: 75% symptoms, 4: death. B) Average disease symptom scores for five commercially available

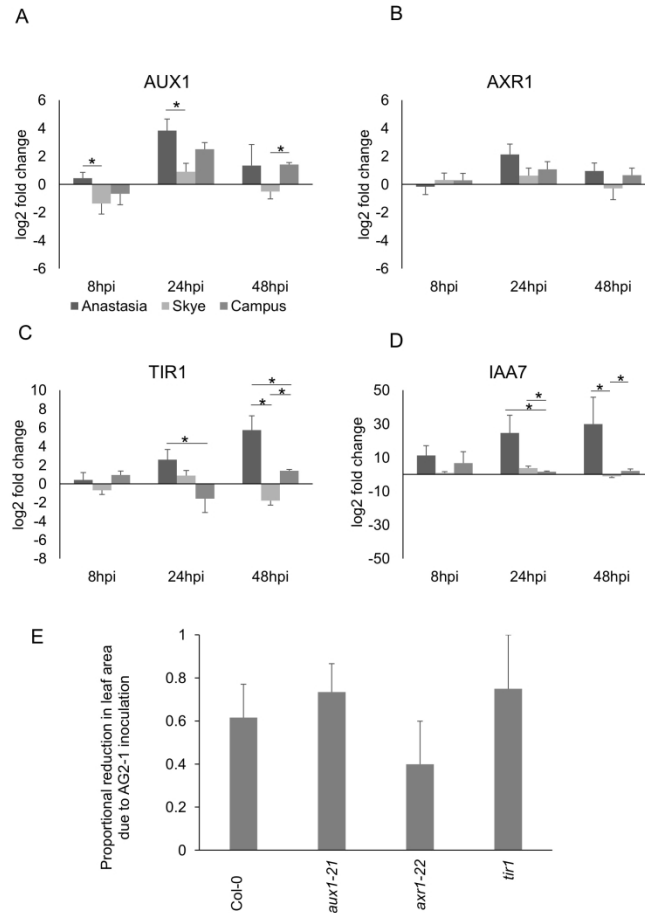
B. napus varieties. Dark grey bars show average hypocotyl symptom scores and light grey bars show average root symptom scores. Non-inoculated data not shown as no individuals showed symptoms. C) Proportional reduction in root length (relative to non-inoculated plant roots) due to AG2-1 measured using ImageJ and SmartRoot plugin. The total length includes lateral roots. Error bars indicate standard error (SE). Different letters above the bars indicated significant differences using t-test, $p < 0.05$.

190x275mm (300 x 300 DPI)



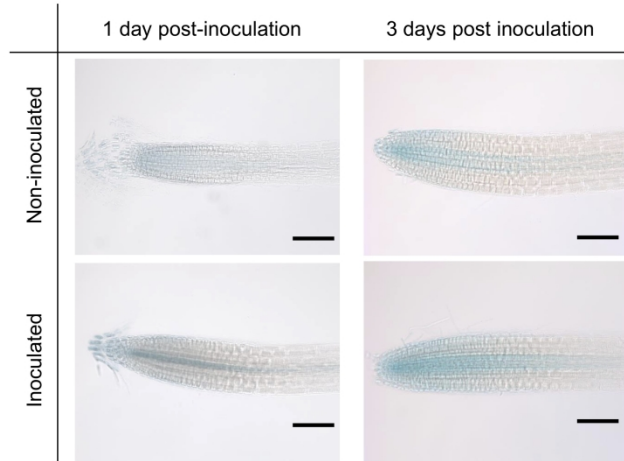
Confocal microscopy images showing *Rhizoctonia solani* AG2-1 sclerotia infection on different *Brassica napus* varieties up to 2 days post-inoculation. Alexa Fluor Wheat Germ Agglutinin 488 and Propidium Iodide staining of fungal tissues and *B. napus* roots, respectively, showing the development of infection structures in Anastasia, Skye, and Campus. Yellow arrowheads indicate infection cushions. Red shows staining with Alexa Fluor Wheat Germ Agglutinin 488. Blue shows staining with Propidium Iodide. The images shown were chosen as representatives from a minimum of nine samples of infected roots for each variety. Scale bar = 250 μ m.

275x190mm (300 x 300 DPI)



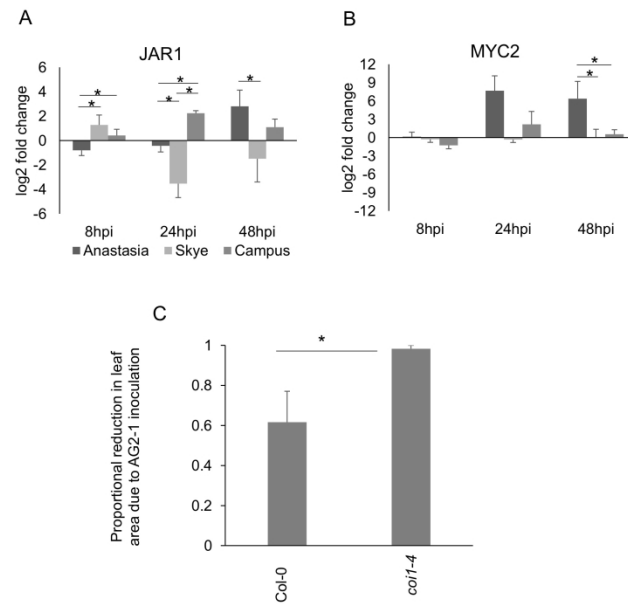
Effect of *Rhizoctonia solani* AG2-1 inoculation on auxin transport and signalling genes (A) AUX1, (B) AXR1, (C) TIR1 and (D) IAA7 in *Brassica napus* varieties Anastasia, Skye and Campus at 8, 24 and 48 hours post inoculation, and (E) proportional reduction in plant leaf area (relative to non-inoculated plants) of *Arabidopsis thaliana* mutant plants at 11 days post inoculation with *Rhizoctonia solani* AG2-1. The data represent log₂ fold change of differential gene expression using non-inoculated plants as internal calibrant. Error bars indicate standard error (SE). Asterisk indicates a significant difference according to Student t test, $p < 0.05$.

190x338mm (300 x 300 DPI)



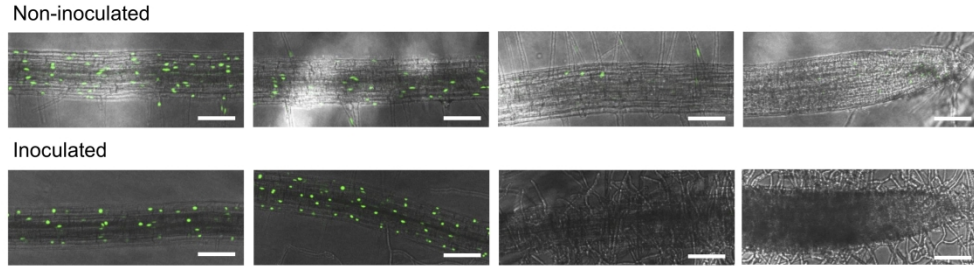
Response of *Arabidopsis thaliana* IAA2pro:GUS lines to *Rhizoctonia solani* AG2-1 at 1 and 3 days post-inoculation. Light microscopy images showing GUS staining in Ws IAA2pro:GUS plants. At the time of sampling, *R. solani* growth had not reached the root of plants. Scale bar = 100 μ m.

275x190mm (300 x 300 DPI)



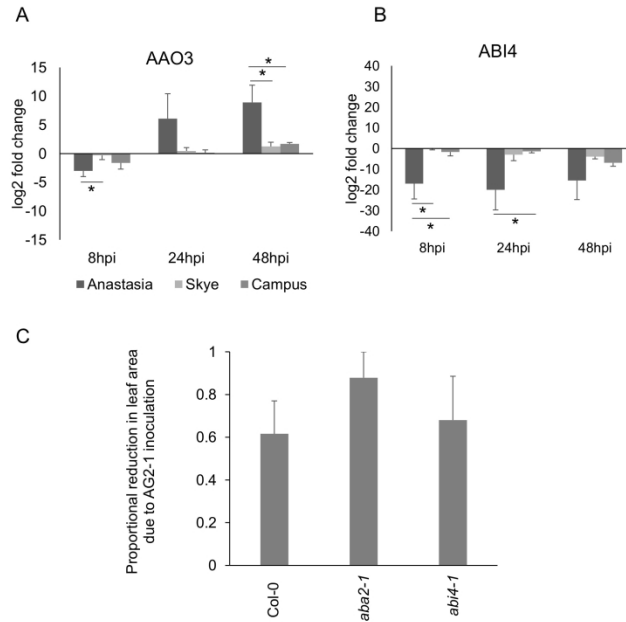
Effect of *Rhizoctonia solani* AG2-1 inoculation on Jasmonic acid signalling genes (A) JAR1 and (B) MYC2 in *Brassica napus* varieties Anastasia, Skye and Campus at 8, 24 and 48 hours post inoculation, and (C) proportional reduction in plant leaf area (relative to non-inoculated plants) of *Arabidopsis thaliana* mutant plants at 11 days post inoculation with *Rhizoctonia solani* AG2-1. The data represent log₂ fold change of differential gene expression using non-inoculated plants as internal calibrant. Error bars indicate standard error (SE). Asterisk indicates a significant difference according to Student t test, $p < 0.05$.

190x338mm (300 x 300 DPI)



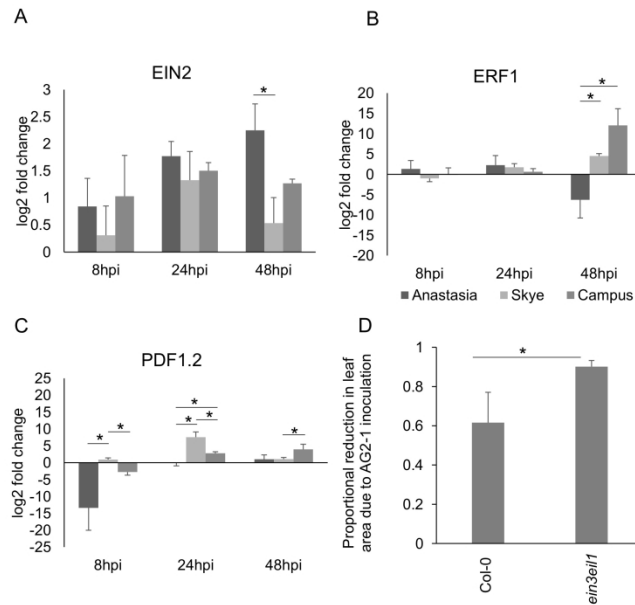
Confocal microscopy images of *Arabidopsis thaliana* Jas9:VENUS seedlings showing Jasmonic acid response to *R. solani* AG2-1 inoculation. Images are ordered left to right reflecting their location within the taproot relative to the root tip, i.e. Farther right is the root tip, and left is furthest from the root tip. Fluorescence from the Jas9:VENUS biosensor is shown in green. Scale bar = 100 μ m.

275x190mm (300 x 300 DPI)



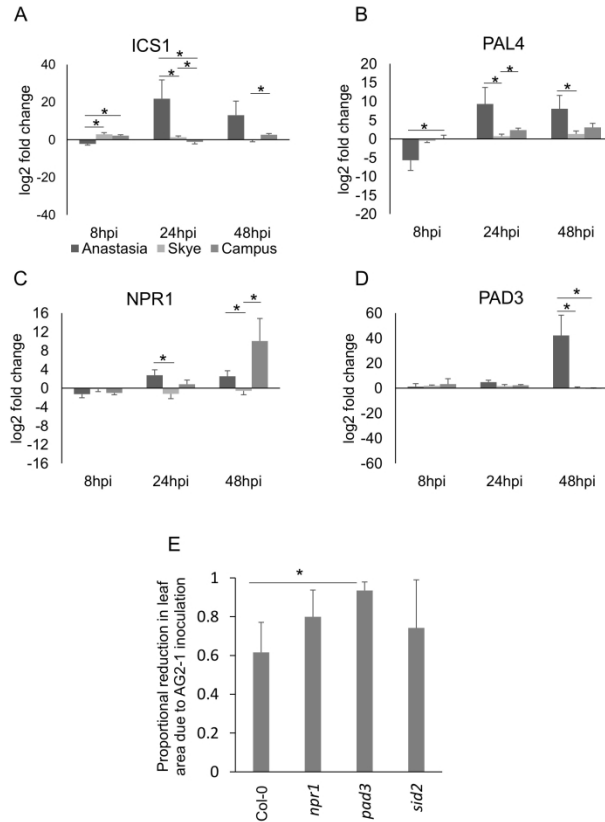
Effect of *Rhizoctonia solani* AG2-1 inoculation on Abscisic acid biosynthesis genes (A) AAO3 and (B) ABI4 in *Brassica napus* varieties Anastasia, Skye and Campus at 8, 24 and 48 hours post inoculation, and (C) proportional reduction in plant leaf area (relative to non-inoculated plants) of *Arabidopsis thaliana* mutant plants at 11 days post inoculation with *R. solani* AG2-1. The data represent log₂ fold change of differential gene expression using non-inoculated plants as internal calibrant. Error bars indicate standard error (SE). Asterisk indicates a significant difference according to Student t test, $p < 0.05$.

190x338mm (300 x 300 DPI)



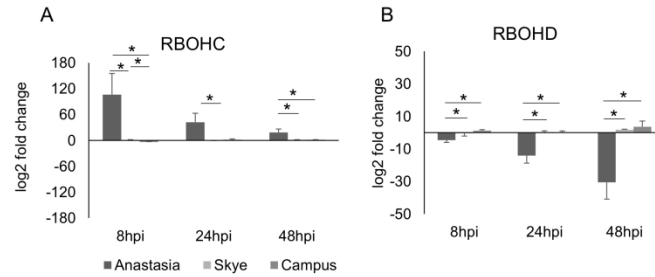
Effect of *Rhizoctonia solani* AG2-1 inoculation on Ethylene signalling genes (A) EIN2, (B) ERF1 and (C) PDF1.2 in *Brassica napus* varieties Anastasia, Skye and Campus at 8, 24 and 48 hours post inoculation, and (D) proportional reduction in plant leaf area (relative to non-inoculated plants) of *Arabidopsis thaliana* mutant plants at 11 days post inoculation with *R. solani* AG2-1. The data represent log₂ fold change of differential gene expression using non-inoculated plants as internal calibrant. Error bars indicate standard error (SE). Asterisk indicates a significant difference according to Student's t test, $p < 0.05$.

190x338mm (300 x 300 DPI)



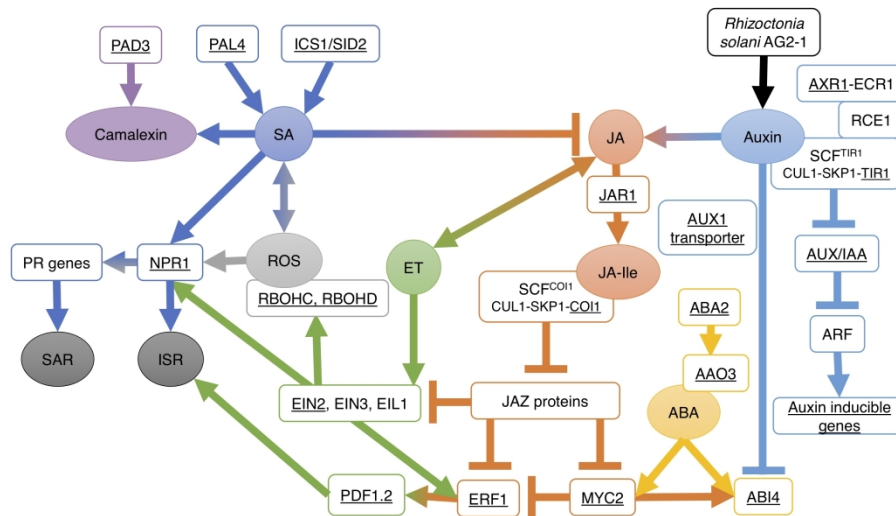
Effect of *Rhizoctonia solani* AG2-1 inoculation on Salicylic acid signalling genes (A) ICS1, (B) PAL4, (C) NPR1 and (D) PAD3 in *Brassica napus* varieties Anastasia, Skye and Campus at 8, 24 and 48 hours post inoculation, and (E) proportional reduction in plant leaf area (relative to non-inoculated plants) of *Arabidopsis thaliana* mutant plants at 11 days post inoculation with *R. solani* AG2-1. The data represent log₂ fold change of differential gene expression using non-inoculated plants as internal calibrant. Error bars indicate standard error (SE). Asterisk indicates a significant difference according to Student's t test, $p < 0.05$.

190x338mm (300 x 300 DPI)



Effect of *Rhizoctonia solani* AG2-1 inoculation on respiratory burst oxidase homologs (RBOHs) genes mediating signal transduction via reactive oxygen species production (A) RBOHC and (B) RBOHD in *Brassica napus* varieties Anastasia, Skye and Campus at 8, 24 and 48 hours post inoculation. The data represent log₂ fold change of differential gene expression using non-inoculated plants as internal calibrant. Error bars indicate standard error (SE). Asterisk indicates a significant difference according to Student t test, $p < 0.05$.

190x338mm (300 x 300 DPI)

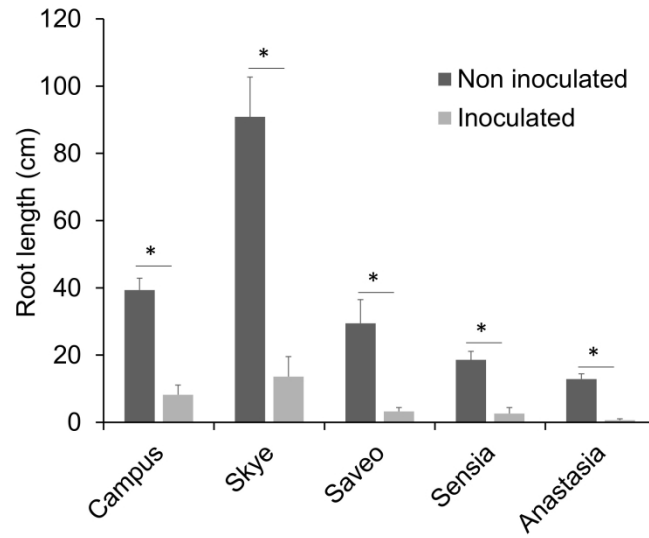


Proposed diagram of hormonal defence pathways involved in the Brassica-*Rhizoctonia solani* AG2-1 interaction. Underlined genes have been tested in this work. Auxin signalling and abscisic acid (ABA) signalling, with the latter likely modified by auxin in compatible interactions, and the MYC2 component of jasmonic acid (JA) signalling together with RBOHC were associated with susceptibility of Brassica hosts to AG2-1 of *R. solani*. In contrast, JA/ethylene (ET) signalling and RBOHD enhanced the defence response to the pathogen. NPR1 functionality dependent on responsive JA/ET defence pathways contributed to induced systemic resistance (ISR) and enhanced defence to AG2-1. In contrast, SAR or ISR by salicylic acid and PAD3 activity were associated with susceptible responses.

275x190mm (300 x 300 DPI)

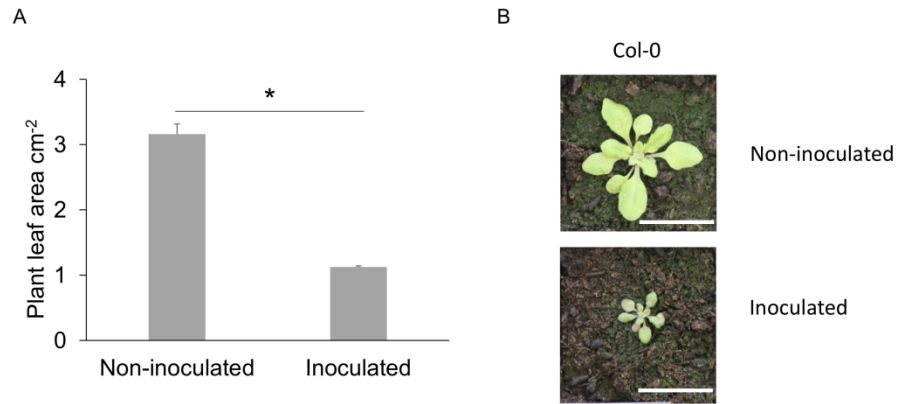
Supplementary Table 1: Primers used for RT-qPCR analysis. All primers were designed using NCBI Primer-BLAST, except the PAL4 primers which were taken from (Zheng *et al.*, 2019).

Gene	Gene name	Forward primer	Reverse primer
AAO3	Abscisic Aldehyde Oxidase 3	TTCCAGCGTGGACTGATGAC	CACTCACATACGGCAATGCG
ABI4	ABA Insensitive 4	GGCCGTTGTTGATCCGGTTA	TTGACCGACCTTTAGGGTTCC
AUX1	Auxin Resistant 1	GCTGCCATCTTCTGGGTTCA	GGGTCCTTTAGTTCTCACTTGC
AXR1	Auxin Resistant 1	TGGCTTGAAGCACAGAGAAGA	CGGCTGAATCGTCCTGAACA
EIN2	Ethylene Insensitive 2	CCAATGGGTTGAAGAAGGACC	GAGGTTTCGACTCTTCGGCT
ERF1	Ethylene Responsive Factor 1	TGTTCAAGTCACCGTTCTCCG	CGGAACGTTTTGCTGTGTGG
IAA7	Indole-3-Acetic Acid 7	TGTTCAACCATATGACGGGTTCT	TCCACACCTCACTGGTAACAT
ICS1	Isochorismate Synthase 1	AGCAACCCAACCTCAGAGTG	ACACACTGATTCTCTATTACCCCA
JAR1	Jasmonate Resistant 1	GGGGAAACAGAGGAGAGACC	CAACGTCACCAAGCCGGTAT
MYC2	MYC2, Jasmonate Insensitive 1	GATTGGAGTACCCGAGCAGG	CCGGATTCCGGTTTTTCGATG
NPR1	Nonexpresser of PR genes 1	CCCGTGATGGTGTACAGAGTT	GTGCATGAACGTTGCCAAC
PAD3	Phytoalexin Deficient 3	TTGGGGATTGCCTGAGAAGG	ACAGCTACCTAAGAATAATACACCC
PAL4	Phenylalanine Ammonia-Lyase 4	GGCACGGACAGTTATGGAGT	GCCGACTTAGGTAGCGTGAG
PDF1.2	Plant Defensin 1.2	CATCACCTTCTCTTCGCTGC	ATGTCCCCTTGACCTCTCGC
RBOHC	Respiratory Burst Oxidase Homolog C	ACTCCGACGCCGAAAGCAG	TTCCGACCCGGGGGATTG
RBOHD	Respiratory Burst Oxidase Homolog D	GACGAGGGAATTCAGGAACC	TTCGTTGTCGGAGTTGGTGT
TIR1	Transport Inhibitor Response 1	TCAACCATGAGGGTTTGCCA	GGGCGATGATGAACAGGATTG



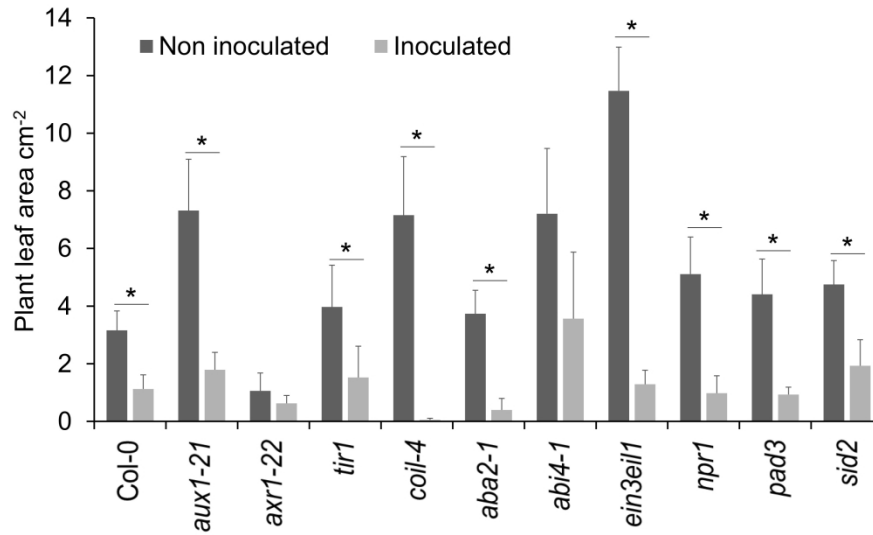
Effect of *Rhizoctonia solani* AG2-1 inoculation on root length (cm) of cvs. Campus, Skye, Saveo, Sensia and Anastasia of *Brassica napus* (oilseed rape). Error bars indicate standard error (SE). Asterisk indicates a significant difference according to Student's t test, $p < 0.05$.

275x190mm (300 x 300 DPI)



Effect of *Rhizoctonia solani* AG2-1 inoculation on (A) plant leaf area of *Arabidopsis thaliana* (Col-0). Images (B) of inoculated and healthy plants shown at 11 days post inoculation. Error bars indicate standard error (SE). Asterisk indicates a significant difference according to Student's t test, $p < 0.05$. Scale bar = 1 cm.

275x190mm (300 x 300 DPI)



Effect of *Rhizoctonia solani* AG2-1 inoculation on plant leaf area of Columbia-0 (Col-0) and mutants of *Arabidopsis thaliana* at 11 days post inoculation. Error bars indicate standard error (SE). Asterisk indicates a significant difference according to Student's t test, $p < 0.05$.

275x190mm (300 x 300 DPI)